Supporting Information

Title: Photophysical properties of three coordinated copper(I) complexes bearing 1,10-phenanthroline and a monodentate phosphine ligand

Authors: Daichi Kakizoe, Michihiro Nishikawa, Yasuo Fujii, Taro Tsubomura*

Table S1. Crystallographic Data for **1-5**

	1	**2**
Formula	$C_{55}H_{52}BCl_2CuF_4N_2P_2$	$C_{60}H_{62}BCuF_4N_2P_2$
Volume	2462.9(8)	2679.7(11)
Temperature, K	123 K	123 K
Cryst syst	triclinic	triclinic
Space group	P -1	P -1
a, Å	12.733(2)	11.685(3)
b, Å	12.864(3)	12.569(3)
c, Å	16.184(3)	20.476(5)
α deg	85.465(5)	90.8113(18)
β deg	69.861(4)	99.2685(19)
γ deg	81.954(5)	114.950(2)
Z	2	2
μ	0.672	0.521
R1, wR2	0.0413, 0.1393	0.0498, 0.1627

	3	**4**	**5**
Formula	$C_{33}H_{29}BCuF_4N_2P$	$C_{32}H_{35}BCuF_4N_2P$	$C_{36}H_{39}BCuF_4N_2P$
Volume	2949.7(10)	1464(7)	3171.3(4)
Temperature, K	123 K	123 K	123 K
Cryst syst	monoclinic	triclinic	monoclinic
Space group	P 1 21/c 1	P -1	P 1 21/n 1
a, Å	11.322(2)	11.05(3)	10.3902(10)
b, Å	17.180(3)	11.05(3)	22.6124(11)
c, Å	15.165(4)	14.68(5)	13.9326(11)
α deg	90.000(4)	106.568(7)	90
β deg	90.000(4)	97.406(6)	104.351(3)
γ deg	90.184(4)	116.748(8)	90
Z	4	2	4
μ	0.846	0.851	0.792
R1, wR2	0.0993, 0.2773	0.0356, 0.1334	0.0318, 0.0769

Table S2 Photophysical data of **3** in degassed CH_2Cl_2.

Complex	λ_{abs} /nm	ε /10^3 $M^{-1}cm^{-1}$	$\lambda_{em, max}$ /nm	τ /μs	Φ
3	389	0.72	610[a]	0.084	-[b]

[a] excited by 390nm [b] Not determined

Table S3 Potential of E_{ox} and E_{red} of **3** in the cyclic voltamograms.

Complex	E_{ox}[a] / V	E_{red} / V
3	0.82	-[b]

[a] Potential of the peak of the oxidation wave. [b] Not determined.

Table S4 The important bond lengths and angles in the singlet optimized structure of **1** and **2**.

Complex	N1-Cu /Å	N2-Cu /Å	P1-Cu /Å	P2-Cu /Å	N1-Cu-N2 /°	P1-Cu-P2 /°
1	2.14561	2.14161	2.30133	2.30532	78.76136	128.50847
2	2.15082	2.13996	2.30254	2.29415	78.56522	124.15544

Table S5 The important bond lengths and angles in the singlet optimized structure of **3**-**5**.

Complex	N1-Cu /Å	N2-Cu /Å	P-Cu /Å	N1-Cu-N2 /°	N1-Cu-P /°	N2-Cu-P /°
3	2.13159	2.03719	2.22765	81.20213	125.95865	152.76765
4	2.11401	2.09034	2.25085	80.46377	129.86539	129.01831
5	2.07079	2.10425	2.22599	81.02754	131.60650	127.51854

Table S6. Result of DFT calculations based on the singlet optimized structures.

Complex	orbital	Energy / eV	Cu[a]	NN[b]	P_{atom}[c]	P_{Ph}[d]	P_{alkyl}[e]	Biaryl[f]
1	LUMO+1	–4.34	0.16	98	0.77	0.3	-	-
	LUMO	–4.41	2.18	96.03	1.06	0.73	-	-
	HOMO	–7.72	45.82	4.83	12.9	36.4	-	-
	HOMO–1	–7.9	63.2	3.73	2.79	30.2	-	-
	HOMO–2	–8.09	81.55	14.39	0.24	3.82	-	-
2	LUMO+1	–4.24	0.1	98.8	0.74	0.33	-	-
	LUMO	–4.32	2.3	95.9	1	0.8	-	-
	HOMO	–7.54	47.6	4.58	12.6	35.2	-	-
	HOMO–1	–7.82	61	3.24	0.44	35.3	-	-
	HOMO–2	–7.98	81.1	14.5	0.1	4.4	-	-
3	LUMO+1	–4.76	0.32	94.02	0	5.7	-	-
	LUMO	–5.00	2.9	94.6	0.29	2.24	-	-
	HOMO	–8.34	64.8	9.5	4.22	21.5	-	-
	HOMO–1	–8.76	50.83	8.24	5.45	35.47	-	-
	HOMO–2	–8.99	5.5	0.43	0.28	93.76	-	-
4	LUMO+1	–4.62	0.18	99.1	0.3	-	0.2	0.19
	LUMO	–4.76	2.26	96.37	0.45	-	0.27	0.64
	HOMO	–8.11	67.98	3.52	4.5	-	7.7	16.3
	HOMO–1	–8.35	76.18	15.32	1.1	-	2.9	4.4
	HOMO–2	–8.76	76.17	5.0	0.19	-	2.95	15.7
5	LUMO+1	–4.59	0.16	99.2	0.35	-	0.14	0.15
	LUMO	–4.74	2.58	96.17	0.34	-	0.23	0.68
	HOMO	–8.1	68.5	4.27	3.57	-	7.9	15.8
	HOMO–1	–8.33	74.8	14.85	1.67	-	3.79	4.87
	HOMO–2	–8.76	76.14	5.03	0.72	-	3.94	14.16

[a] Components moiety of the copper atom (%). [b] Components moiety of the diimine ligand (%). [c] Components moiety of the phosphorus atom (%). [d] Components moiety of the monodentate phosphine ligand except the phosphorus atom (%). [e] Components moiety of the alkyl group (%). [f] Components moiety of the biaryl unit (%)

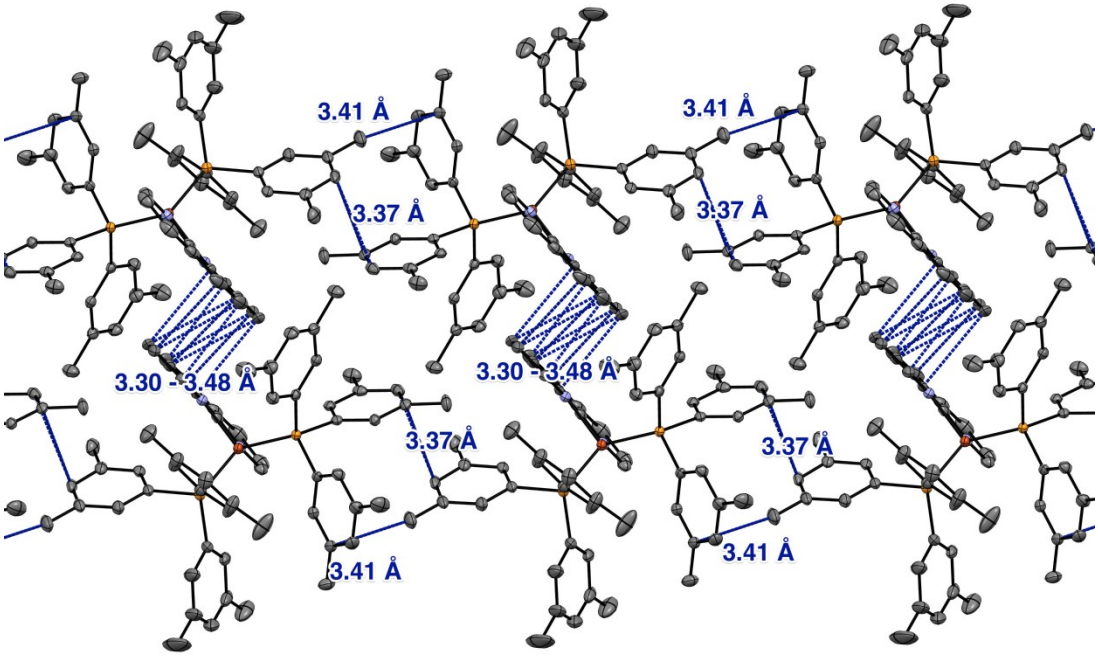

Fig. S1. Intermolecular interactions in the crystal of **2**.

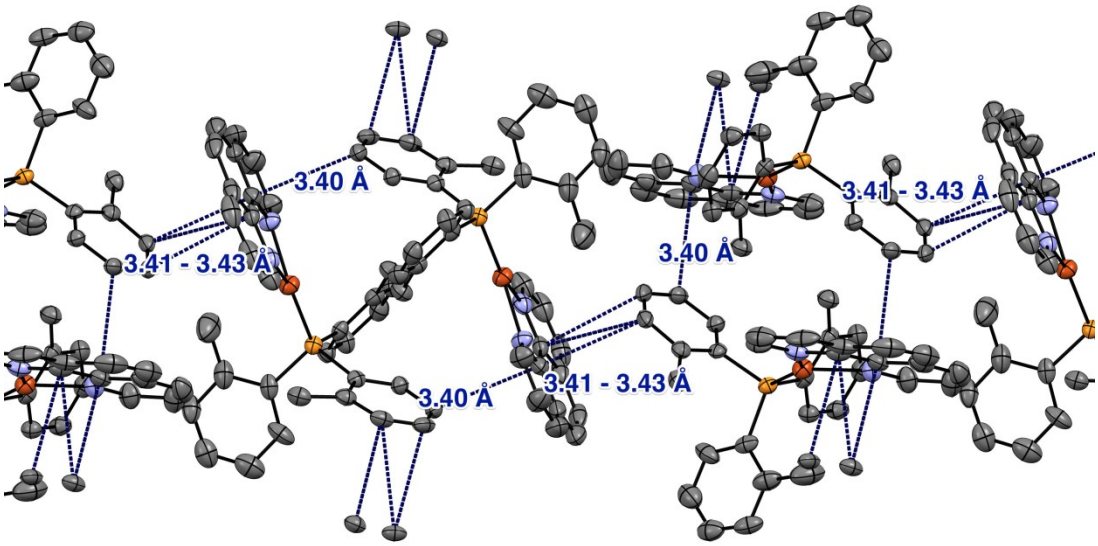

Fig. S2. Intermolecular interactions in the crystal of **3**.

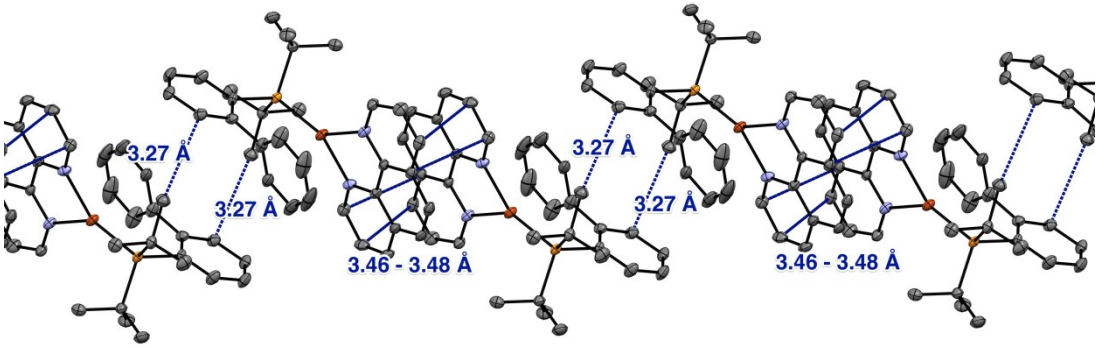

Fig. S3. Intermolecular interactions in the crystal of **4**

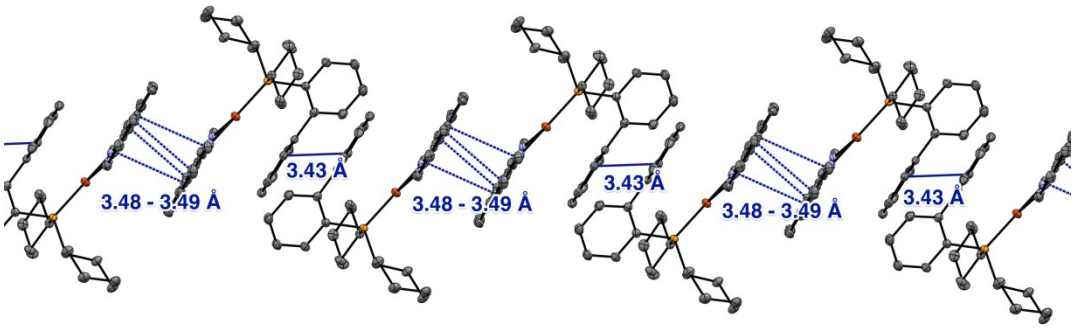

Fig. S4. Intermolecular interactions in the crystal of **5**.

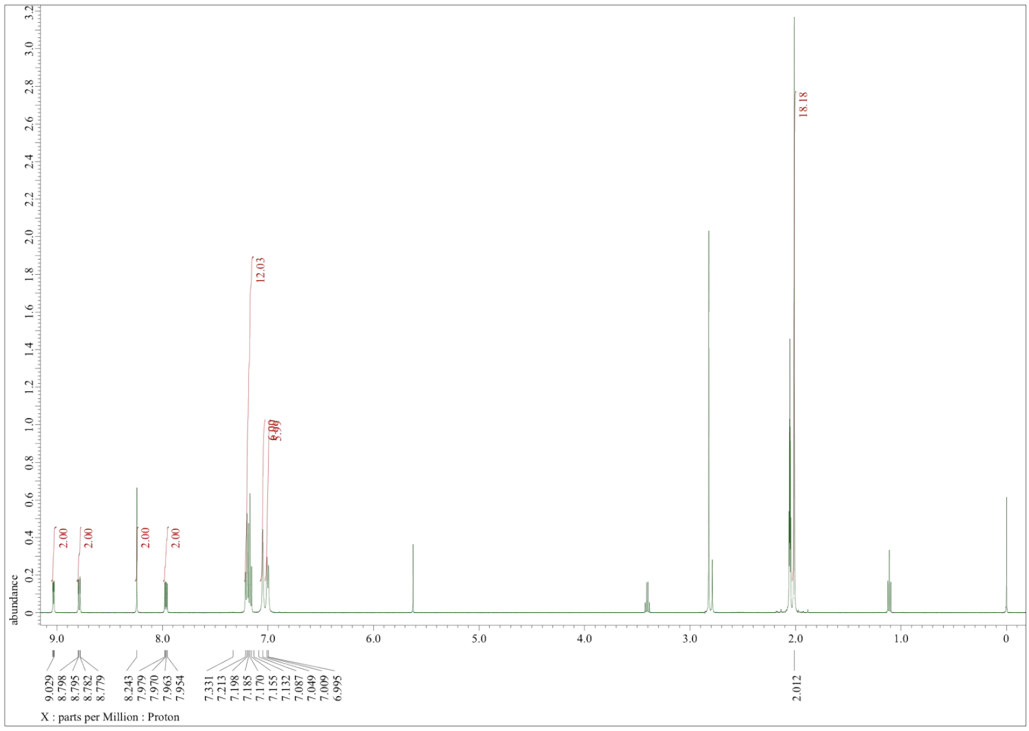

Fig. S5. ^{1}H NMR spectrum of **1** in acetone-d_6 at room temperature.

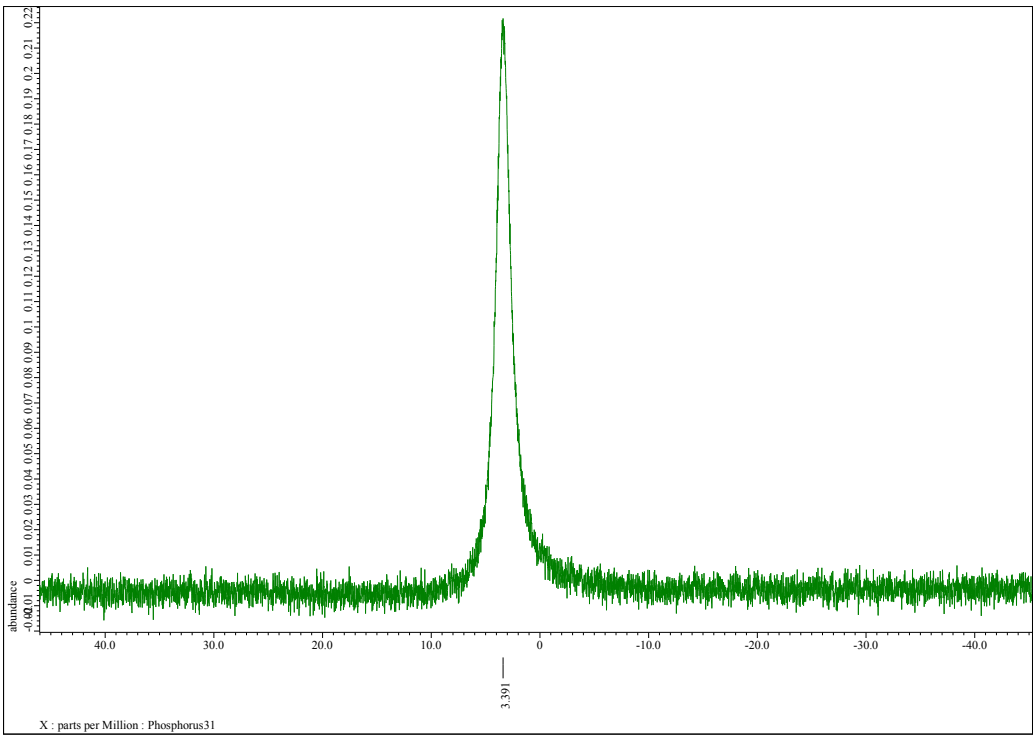

Fig. S6. ^{31}P{^{1}H} NMR spectrum of **1** in acetone-d_6 at room temperature

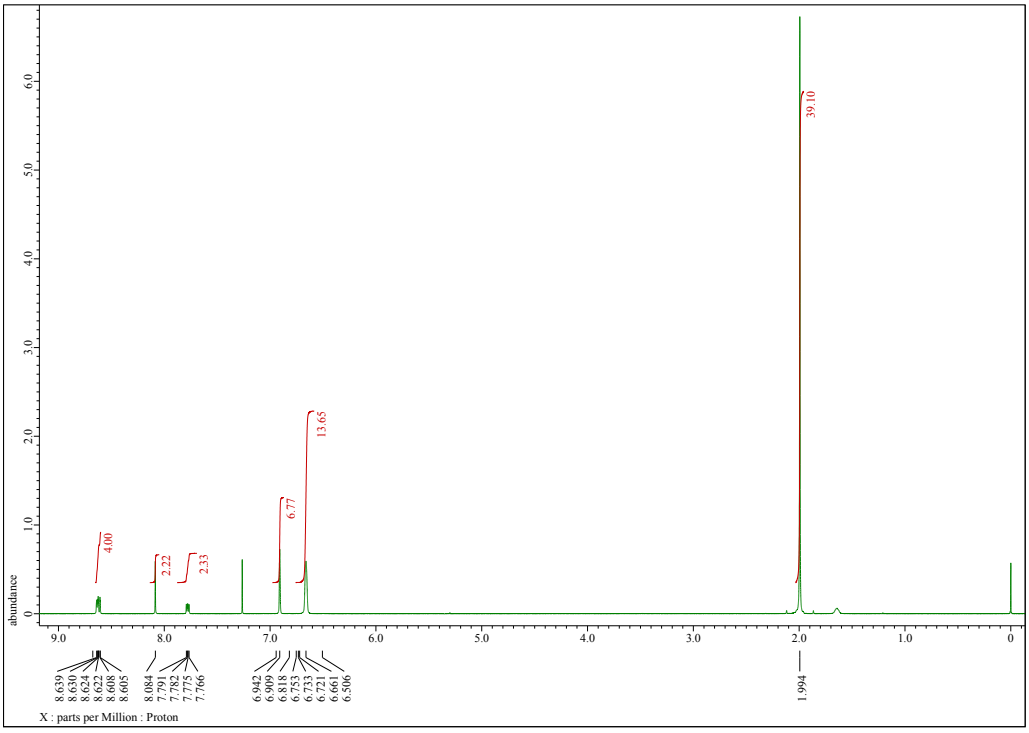

Fig. S7. ^{1}H NMR spectrum of **2** in $CDCl_3$ at room temperature.

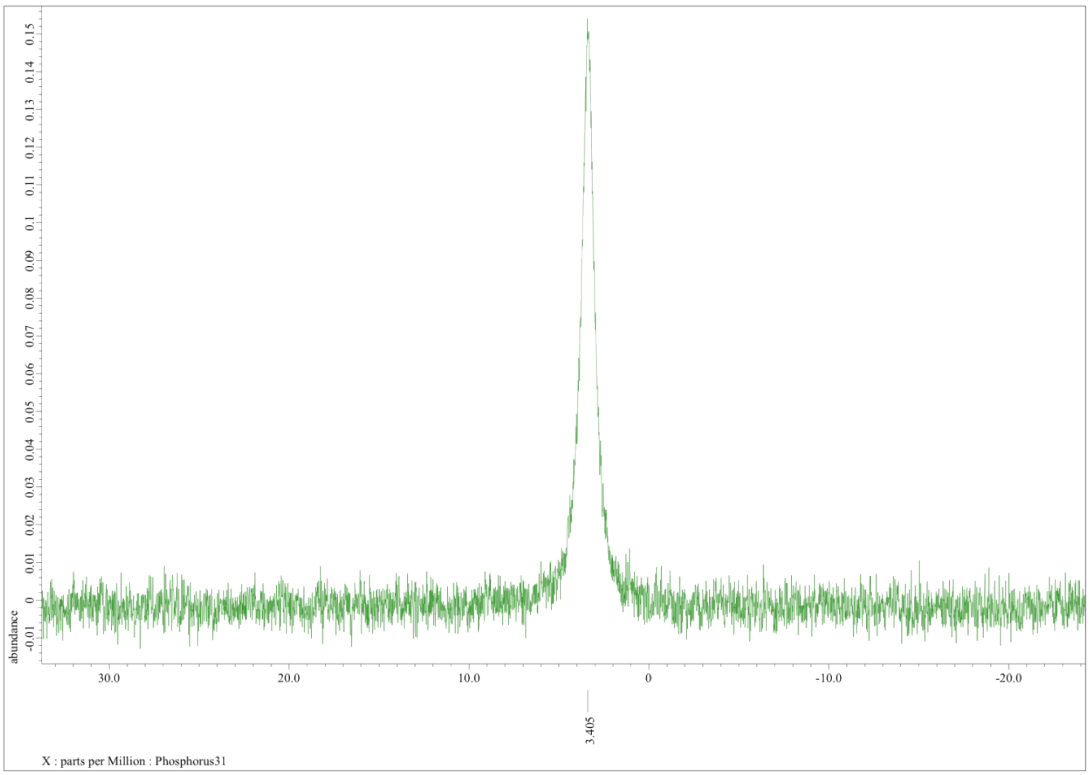

Fig. S8. ^{31}P{^{1}H} NMR spectrum of **2** in $CDCl_3$ at room temperature

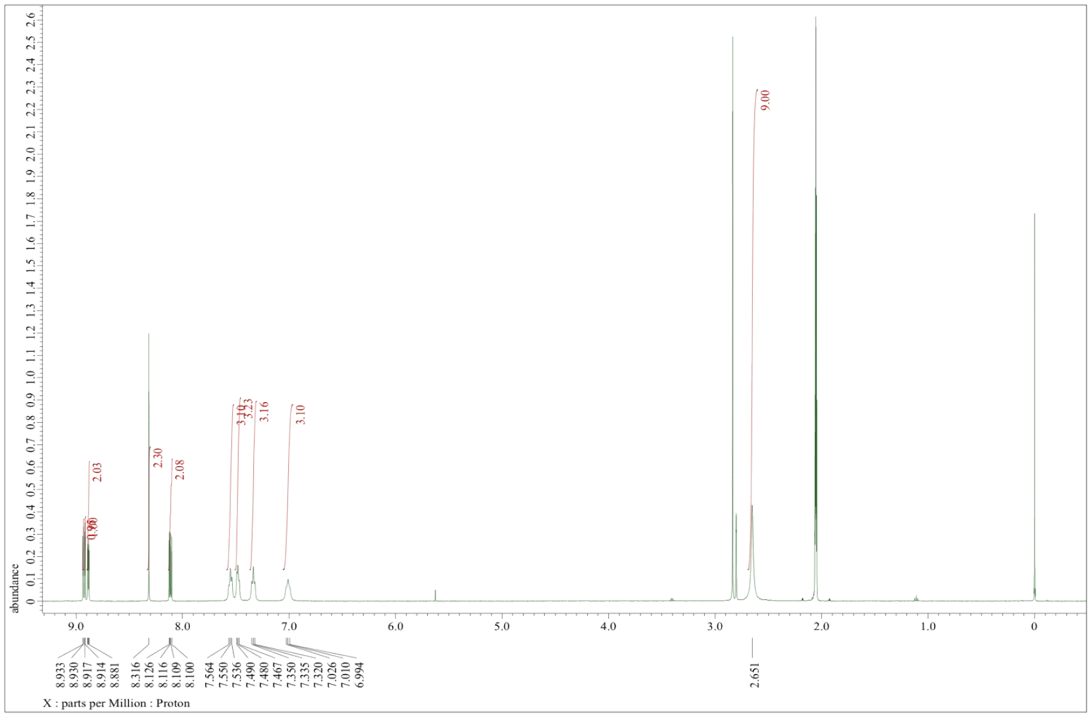

Fig. S9. ^{1}H NMR spectrum of **3** in acetone-d_6 at room temperature.

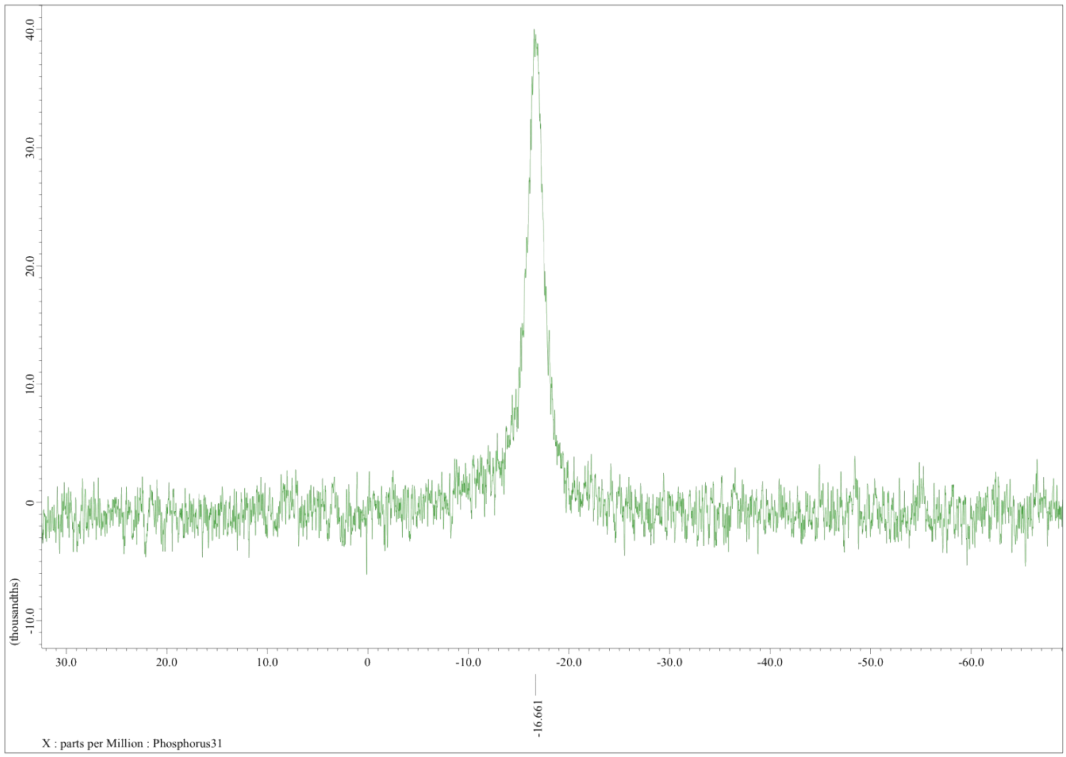

Fig. S10. ^{31}P{^{1}H} NMR spectrum of **3** in acetone-d_6 at room temperature.

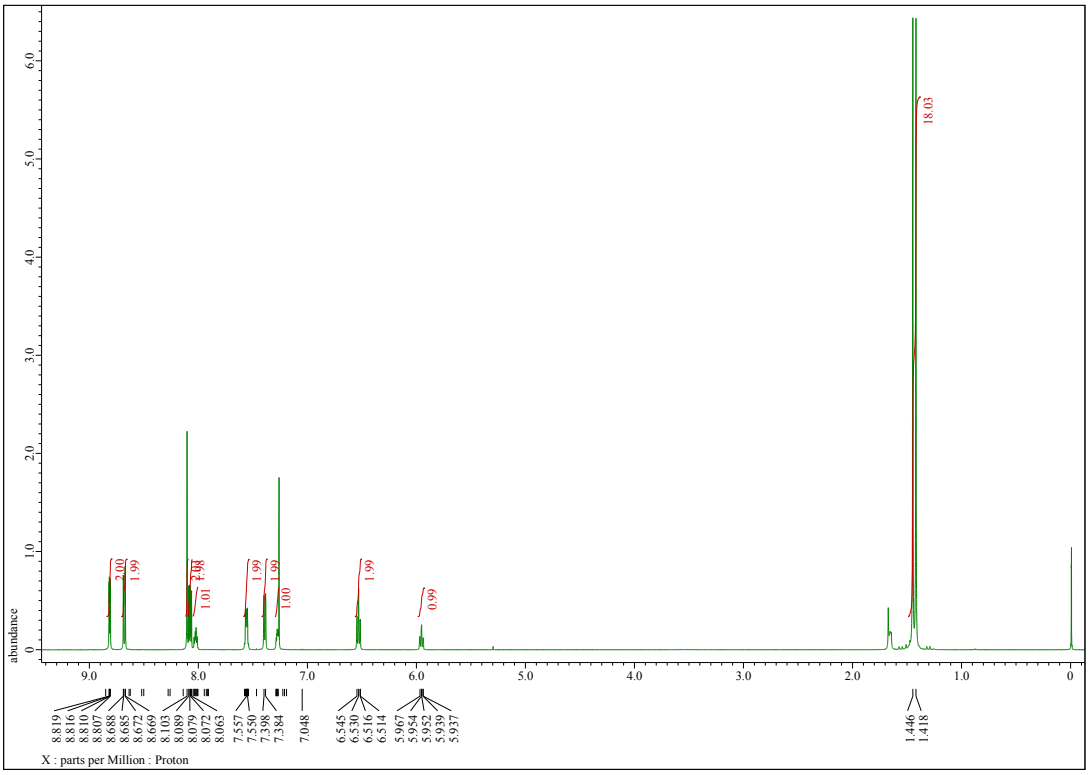

Fig. S11. ^{1}H NMR spectrum of **4** in $CDCl_3$ at room temperature.

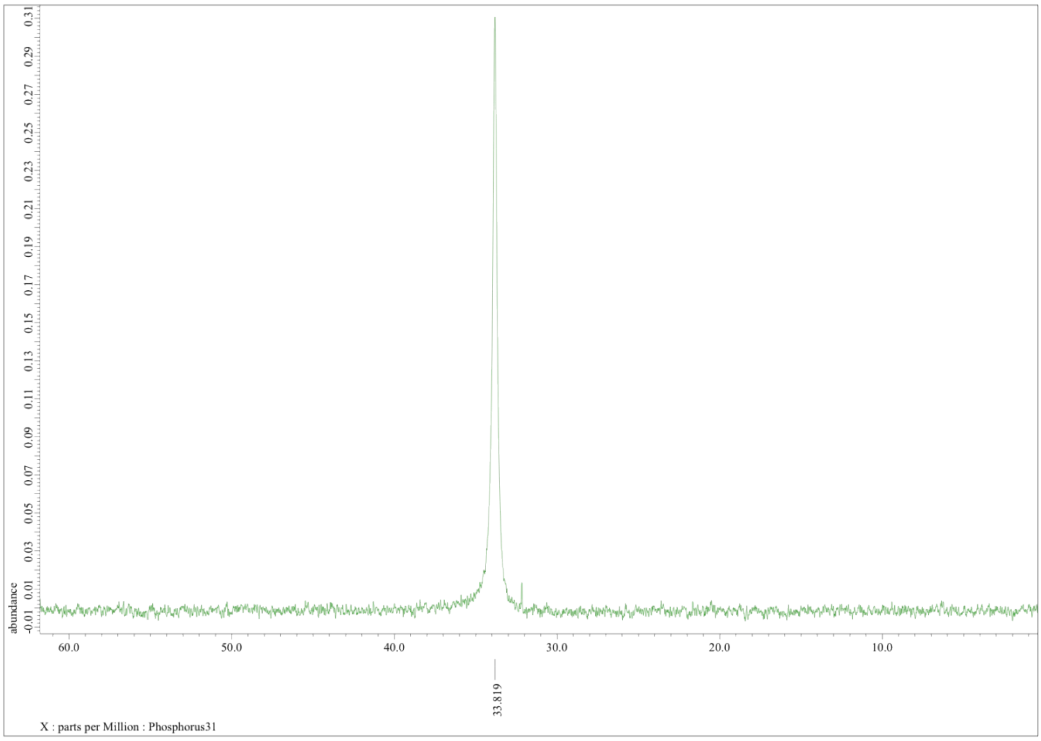

Fig. S12. ^{31}P{^{1}H} NMR spectrum of **4** in $CDCl_3$ at room temperature.

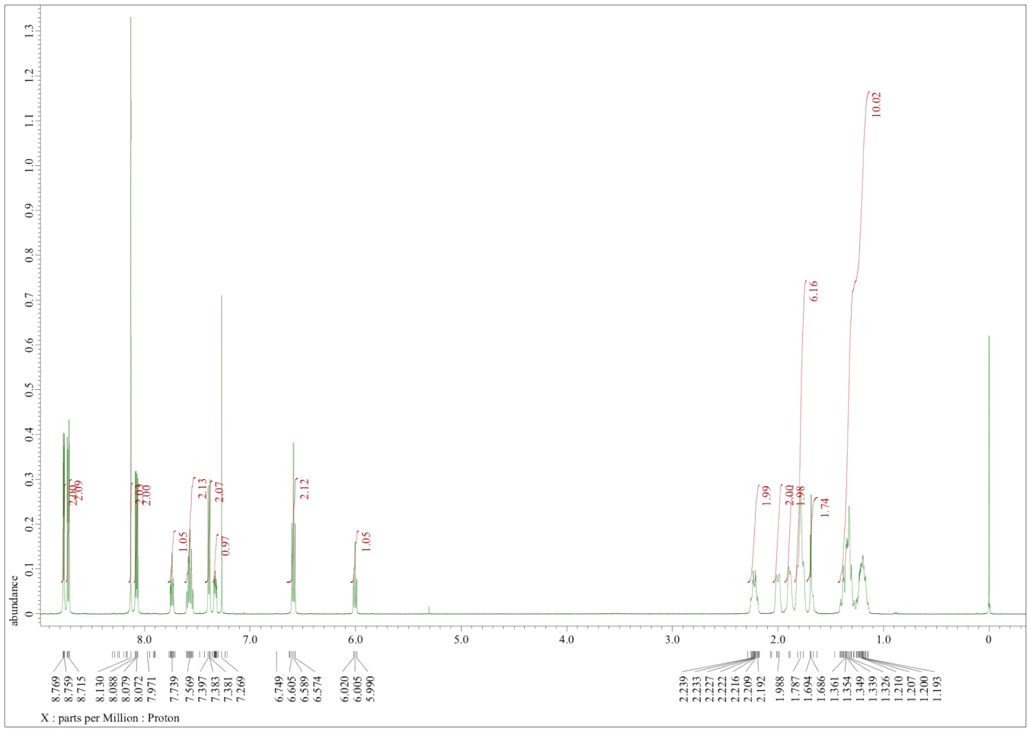

Fig. S13. ^{1}H NMR spectrum of **5** in $CDCl_3$ at room temperature.

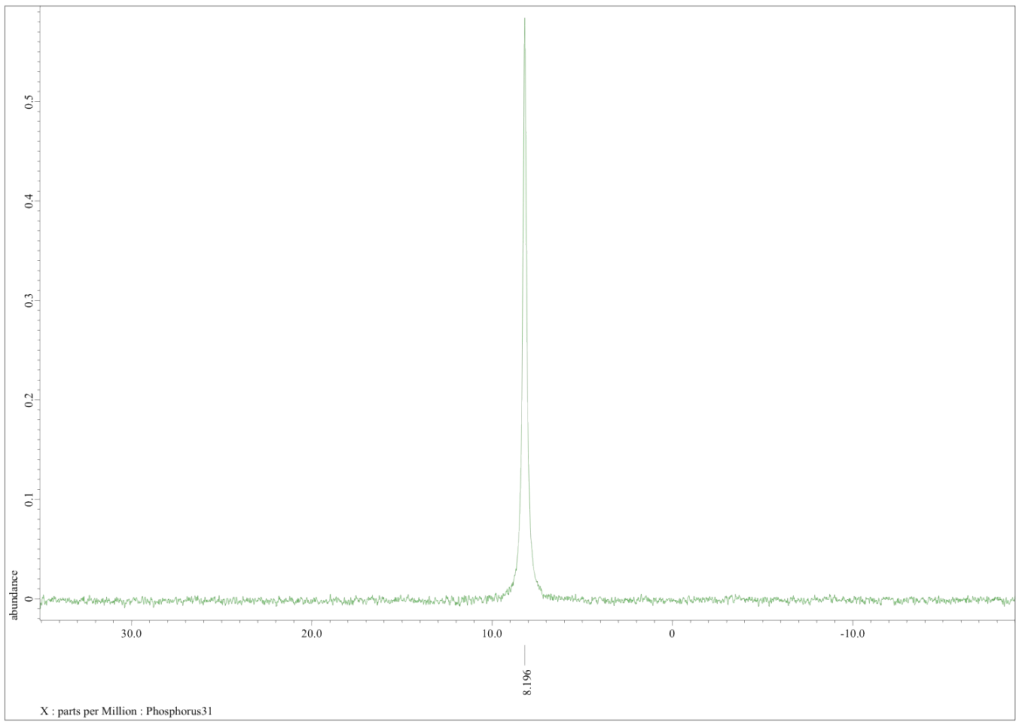

Fig. S14. ^{31}P{^{1}H} NMR spectrum of **5** in $CDCl_3$ at room temperature.

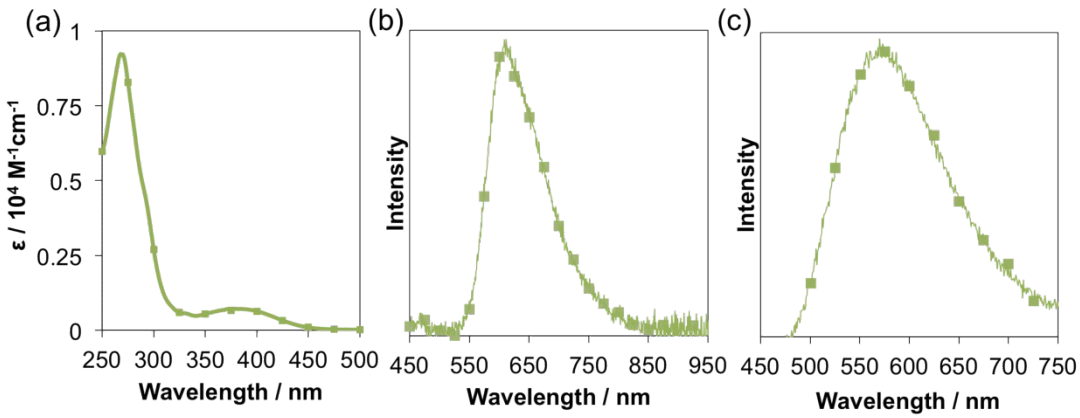

Fig. S15 (a) Absorption spectrum of **3** in CH_2Cl_2 (b) Emission spectrum of **3** in degassed CH_2Cl_2 at room temperature. (c) Emission spectrum of **3** in the solid state.

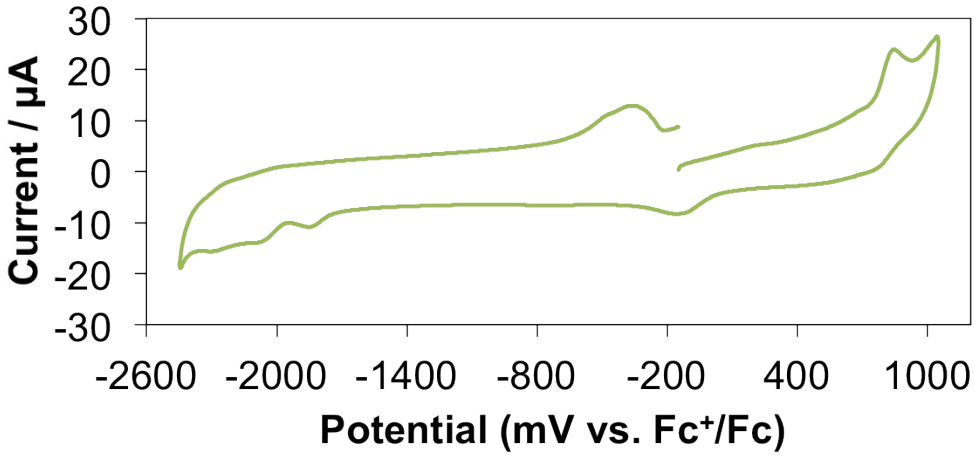

Fig. S16 Cyclic voltammogram of 0.5mM of **3** in degassed 0.1M $TBAPF_6$–acetone at room temperature at the scan rate of 0.2 Vs^{-1}.

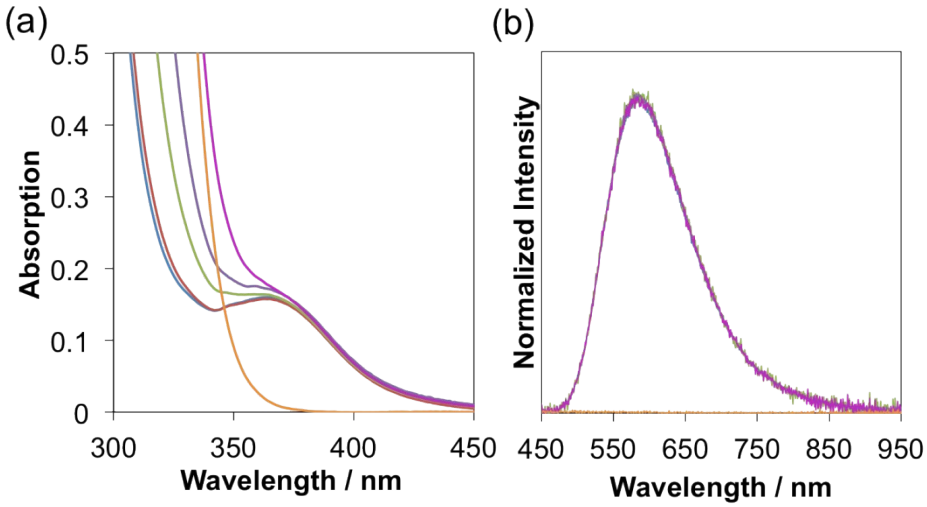

Fig. S17. (a) Absorption spectra of **4** (7.63×10^{-5} mol/L, blue), the ligand (7.65×10^{-3} mol/L, orange) and the mixture of **4** and the ligand in the ratio of 1:2.5(red), 1:11(green), 1:25(purple) and 1:95(magenta) in CH_2Cl_2 at room temperature. (b) Emission spectra of **4**(7.63×10^{-5} mol/L, blue), the ligand (7.65×10^{-3} mol/L, orange) and the mixture of **4** and the ligand in the ratio of 1:2.5(red), 1:11(green), 1:25(purple) and 1:95(magenta) in CH_2Cl_2 in degassed CH_2Cl_2 by 20 min argon bubbling.

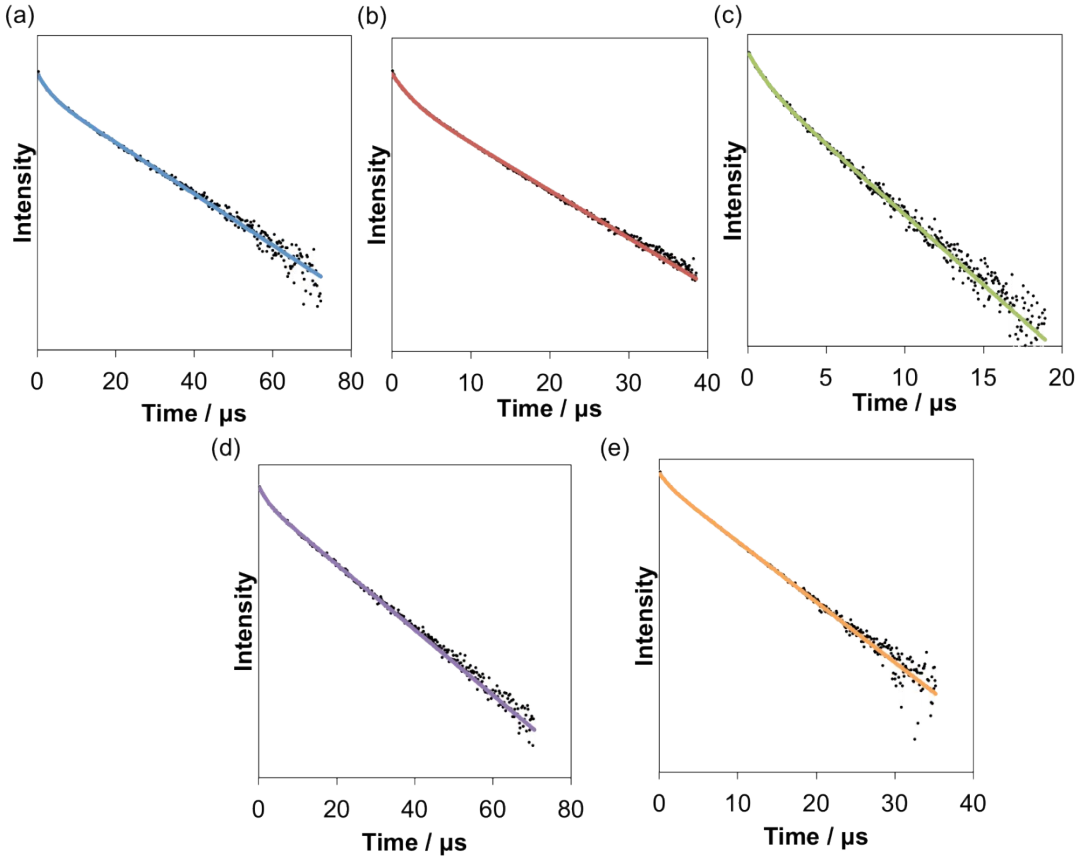

Fig. S18. The emisson decay curves of **1** (a, blue), **2** (b, red), **3**(c, green), **4**(d, purple) and **5**(e, orange) in the solid state. The colored solid line in the figures represent the fitted curves with double exponential functions.

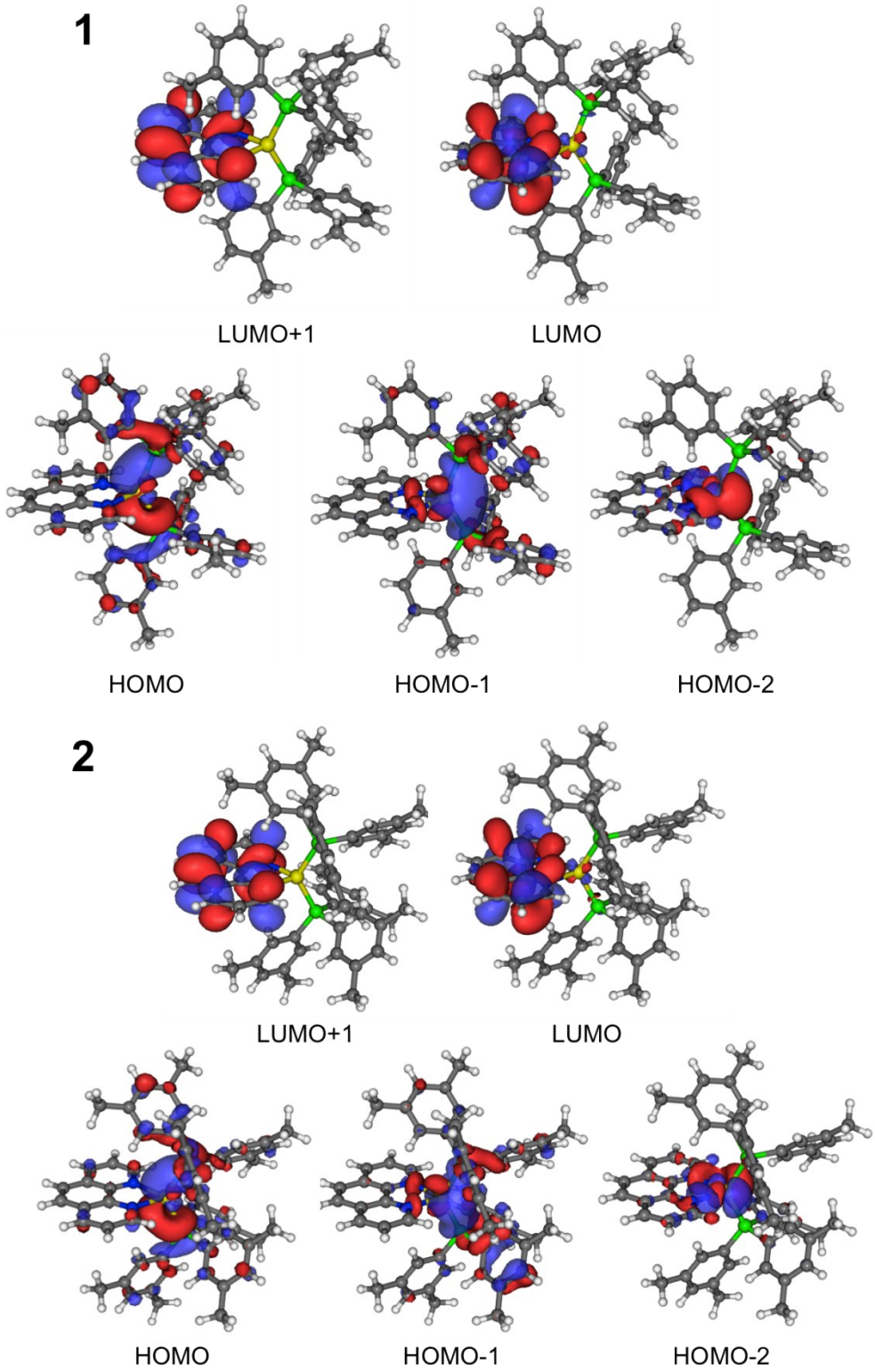

Fig. S19. Calculated Kohn-Sham orbitals of **1** and **2** in the singlet optimized structure. (Isosurface value, 0.02)

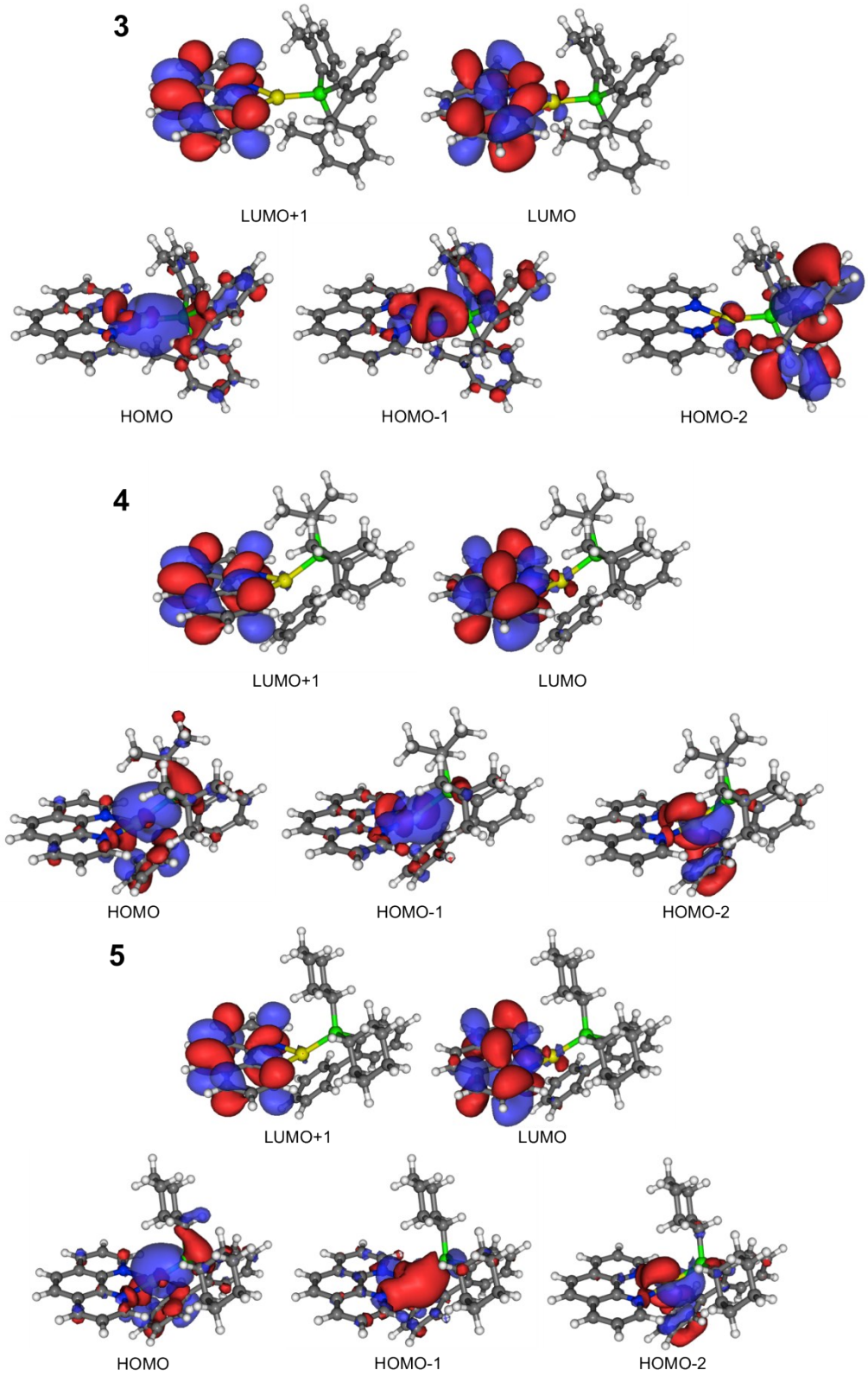

Fig. S20. Calculated Kohn-sham orbitals of **3-5** in the singlet optimized structure. (Isosurface value, 0.02)